Fusion between Retinal Rod Outer Segment Membranes and Model Membranes: A Role for Photoreceptor Peripherin/rds†

Kathleen Boesze-Battaglia,*,‡ Om P. Lamba,§ Andrew A. Napoli, Jr.,‡ Santosh Sinha,§ and Yuqing Guo‡,||

Department of Molecular Biology, University of Medicine and Dentistry of New Jersey-SOM, 2 Medical Center Drive, Stratford, New Jersey 08084, and Department of Ophthalmology and Visual Sciences, University of Louisville School of Medicine, Louisville, Kentucky 40292

Received January 23, 1998; Revised Manuscript Received May 6, 1998

ABSTRACT: Peripherin/rds plays an essential role in the maintenance of photoreceptor rod cell disk membrane structure. The purification of this protein to homogeneity [Boesze-Battaglia, K., et al. (1997) *Biochemistry 36*, 6835−6846] has allowed us to characterize the functional role of peripherin/rds in the maintenance of rod outer segment (ROS) membrane fusion processes. Utilizing a cell-free fusion assay system, we report that the fusion of R_{18}-labeled ROS plasma membrane (R_{18}-PM) with disk membranes or peripherin/rds-enriched large unilammellar vesicles (LUVs) is inhibited upon trypsinolysis of peripherin/rds. To understand this phenomenon, we tested the ability of a series of overlapping synthetic C-terminal peripherin/rds peptides to mediate model membrane fusion. Within the 63 amino acid long region of the C-terminus, we identified a minimal 15 residue long amino acid sequence (PP-5), which is necessary to promote membrane fusion. PP-5 was able to inhibit R_{18}-PM disk membrane fusion and promoted ANTS/DPX contents mixing in a pure vesicle system. This peptide (PP-5) promoted calcium-induced vesicle aggregation of phosphatidylethanolamine:phosphatidylserine LUVs. FTIR analysis confirmed the structural prediction of this peptide as α-helical. When modeled as an α-helix, this peptide is amphiphilic with a hydrophobicity index of 0.75 and a hydrophobic moment of 0.59. PP-5 has substantial biochemical and functional homology with other well-characterized membrane fusion proteins. These results demonstrate the necessity for peripherin/rds in ROS membrane fusion, specifically the requirement for an intact C-terminal region of this protein.

Membrane fusion processes are involved in diverse cellular responses, including endocytosis, exocytosis, viral infection, secretion, and fertilization (for review, see ref *1*). A number of common mechanistic themes have evolved from the study of intracellular fusion, model membrane fusion and viral and cell−cell fusion. A commonality among most of these fusion processes is the presence of a fusion protein or proteins to regulate and mediate this process (for review see ref *2*). These proteins are postulated to aid in the thermodynamically unfavorable fusion event by promoting hydrophobic interactions that favor fusion. Such fusion proteins are most often integral membrane proteins that change conformation so as to expose a hydrophobic domain that promotes the mixing of two opposing bilayers (*2*). A typical structural feature of viral fusion proteins and PH-30 (*3*) for example, is the presence of short fusion peptides generally 16−26 amino acids in length. These fusion peptides are characterized by their high hydrophobicity; modeling studies show that they form amphiphilic α-helical structures (*4*) composed of a hydrophobic face and a back with high hydrogen-bonding capacity (*5*−*7*). Most of these peptides are oriented obliquely within the opposing bilayer (*6*) and destabilize the target membrane (*2*, *5*, *8*−*10*) and/or host membranes (*11*−*15*). Fusion peptides are part of a membrane anchored domain and may be internal to the polypeptide chain (*2*).

A system in which fusion processes have yet to be clearly defined is the rod photoreceptor cell. These cells are responsible for vision under dim light. The initial biochemical events which ultimately culminate in phototransduction occur within the rod outer segment (for review see ref *16*). The ROS[1] contains a stack of closed flattened membranous sacs referred to as disks. The organization of individual disks in a discontinuous lateral array distinguishes these cells from cones. The length of the ROS remains constant through the coordinated processes of disk membrane formation (at base) and disk shedding (at tip). New disk closure (*17*) and disk membrane packet formation prior to shedding (*18*) are considered to involve tightly controlled membrane fusion processes. Thus, at two clearly defined locations (the base and tip of ROSs), membrane fusion must occur for the rod

† This work was supported by NEI EY10420 (KBB) and EY10245 and partially by Research to Prevent Blindness (OPL).

* Author to whom correspondence should be addressed. Phone: (609) 566-6194. Fax: (609) 566-6232. E-mail: battagli@umdnj.edu.

‡ University of Medicine and Dentistry of New Jersey School of Osteopathic Medicine.

§ University of Louisville School of Medicine.

|| Present address: Biomira-USA 1002 Eastpack Blvd. Cranbury, NJ 08512.

[1] Abbreviations: ROS, rod outer segment; OG, octylglucopyranoside; Con-A, Concanavalin-A, R_{18}, octadecylrhodamine B chloride; PC, phosphatidylcholine; PE, phosphatidylethanolamine; *N*-methyl-DOPE, *N*-methyl dioleoyl phosphatidylethanolamine; PS, phosphatidylserine; LUVs, large unilammellar vesicles; IRF, initial rate of fusion; ANTS, 1-aminonaphthalene-3,6,8-trisulfonic acid; DPX, *p*-xylylenebis(pyridinium bromide); R_{18}-PM, R_{18}-labeled plasma membrane vesicles.

S0006-2960(98)00173-1 CCC: $15.00
Published on Web 06/11/1998

cell to maintain an ordered array of disks and physiological function. Such membrane fusion is supported by microscopic studies illustrating perturbations of ROS membrane structure in the form of vesiculation and tubulation (*19*−*21*). Investigators have also shown that the aqueous interior of some disks becomes continuous with the external medium during packet formation (*22*, *23*). Fluorescence microscopy using Lucifer yellow labeling revealed the intrusion of dye specifically in the region of packet detachment in the ROS during shedding. The Lucifer yellow staining was localized to single or multiple bands across the ROS and did not spread throughout the entire ROS. It was suggested that the restraint of staining to relatively narrow bands was due to fusion between only selected ROS disks and the plasma membrane (*23*). To study these fusion processes biochemically, we have developed an in vitro cell-free system to characterize which factors may regulate fusion between disk and the plasma membrane (*18*, *24*, *25*). Using the well-characterized R_{18} lipid mixing assay, we have identified various cofactors, including calcium (*18*) and retinal/retinol (*25*) that modulate fusion between disk membranes and isolated plasma membrane vesicles.

Recent work linking retinal degenerations to the peripherin/rds gene and the morphological characteristics of this disease has focused our attention on the potential role of peripherin/rds in membrane fusion processes in the ROS. The cDNA for peripherin/rds has been cloned and codes for a 39 kDa integral membrane glycoprotein with four putative transmembrane domains (*26*, *27*). In the retinal degeneration slow (*rds*) mouse model of retinal degeneration, a single mutation results in the deletion of the C-terminus of peripherin/rds (*26*). *rds* mouse homozygotes exhibit abnormal disk membrane morphogenesis; ROSs do not develop, and the photoreceptor cells eventually die (*28*, *29*). Transgenic rescue with a normal copy of the *rds* gene results in the formation of normal ROSs and no morphological indication of photoreceptor degenerations (*30*). Interestingly, *rds* heterozygotes do exhibit aberrant disk shedding (*31*, *32*). The mechanism by which mutations in peripherin/rds result in retinal degeneration is unknown.

On a molecular level, peripherin/rds has been localized to the rim region of the disk membranes (*33*). This is the same region that must come in contact with and ultimately fuse with the plasma membrane. Within this rim region, peripherin/rds forms a noncovalent−heterotetrameric complex with rom-1, a nonglycosylated homologue (*34*−*36*). Molday and his colleagues (*37*−*39*) have proposed that these proteins function as a multimeric unit. These conclusions were based on studies in native disk membranes, in which peripherin/rds forms a complex with rom-1 and in a COS cell expression system, in which peripherin/rds is abnormally glycosylated (*37*). The purification of bovine peripherin/rds to homogeneity has allowed us to propose a novel functional role for peripherin/rds (*40*). Using native purified peripherin/rds, reconstituted into disk lipid vesicles, we have shown that this protein promotes membrane fusion in an in vitro system (*40*). Peripherin/rds stimulated fusion occurs in the absence of rom-1 and is increased by phosphorylation (*40*). In the present study, we have continued to characterize the role of peripherin/rds in fusion by identifying a fusion promoting region of this protein.

The evidence presented herein shows that synthetic peptide mimicking regions of the C-terminal region of peripherin/rds regulate in vitro fusion between isolated plasma membrane vesicles and disk membranes. A specific region of the C-terminal domain contains a fusogenic peptide that promotes aqueous contents mixing. This sequence can be modeled as a sided α-helix. This growing body of evidence supports the hypothesis that peripherin/rds is a likely fusion protein in photoreceptor cells and the first such protein to be identified in this cell type.

EXPERIMENTAL PROCEDURES

Materials. Frozen, dark-adapted bovine retinas were purchased from J. Lawson Inc., Lincoln, NE. Monoclonal antibodies, 2B6, against peripherin/rds, and 1D5, against rom-1, were given to us as hybridoma culture media by Dr. R. Molday. PBE-94 and polybuffer were purchased from Pharmacia. Concanavalin-A (Con-A) Sepharose and octylglucopuranoside (OG) were purchased from Calbiochem (La Jolla, CA). R_{18}:octadecylrhodamine B chloride (R_{18}), 1-aminonaphthalene-3,6,8-trisulfonic acid (ANTS), and *p*-xylylenebis(pyridinium bromide) (DPX) were purchased from Molecular Probes (Eugene, Or). Phosphatidylethanolamine (PE), *N*-methyl dioleoyl phosphatidylethanolamine (*N*-methyl-DOPE) phosphatidylserine (PS, bovine brain) and phosphatidylcholine (PC, egg) were purchased from Avanti Polar Lipids (Atlanta, GA). All other chemicals were purchased from Sigma (St. Louis, MO).

Peptides corresponding to overlapping regions of the C-terminal region of peripherin/rds (peptides designated PP-3 to PP-7) and an N-terminal peptide (NP-1) were synthesized by Quality Control Biochemical (QCB). PP-2, to the first intradiskal loop of peripherin/rds, was synthesized by Research Genetics (Huntsville, AL). Mass spectrometry confirmed peptide purity of 95%.

The amino acid sequence of NP-1 is H_2N-A-L-L-K-V-K-F-D-Q-K-K-R-V-COOH, corresponding to amino acid residues 1−13 of bovine peripherin/rds (*27*). The amino acid sequence of PP-2 is H_2N-R-K-R-S-D-V-M-N-N-S-D-S-H-F-V-COOH, corresponding to amino acid residues 45−60 of bovine peripherin/rds (*27*).

Rod Outer Segment Membrane Preparations. Retinal ROS disk membranes were prepared from frozen, dark-adapted retinas (J. Lawson Inc., Lincoln, NE) (*41*). The isolated ROS disk membranes were washed in hypotonic buffer, 5 mM Hepes and 1 mM EDTA, pH 7.8, twice to remove soluble proteins prior to Con-A chromatography. Leupeptin (10 μM) and aprotinin (1 μM) were included in all of the isolation buffers. All manipulations of ROS membranes were performed under dim red light, and all buffers were purged with argon to reduce lipid oxidation.

Concanavalin A Affinity Chromatography. Con-A chromatography was carried out at room temperature under dim red light (*42*). Hypotonically washed ROS disk membranes were suspended in Con-A standard buffer and solubolized in OGL (*42*). Fractions were monitored at 280 nm, and peak fractions corresponding to the flow through were pooled and are designated as the unbound fraction described previously (*40*). The rhodopsin-rich protein fractions (eluted with 0.5 M α-methylmannoside) were also pooled and are designated the bound fraction as described (*40*). The

Table 1: Aligned Amino Acid Sequence of Synthetic C-Terminal Peripherin/rds Peptides from the Amino to the Carboxyl Terminal (Left to Right) is Shown[a]

peptide	amino acid sequence
PP-3	V-E-A-E-G-E-D-A-G-Q-A-P-A-A-G
PP-4	S-V-K-K-L-G-K-G-N-Q-V-E-A
PP-5	V-P-E-T-W-K-A-F-L-E-S-V-K-K-L
PP-6	L-K-S-V-P-E-T-W-K-A-F-L
PP-7	W-K-A-F-L
Residue #	H_2N-308------311--------315----------321----------331----------345-COOH

[a] The corresponding residue numbers are indicated at the bottom.

unbound fraction was concentrated by Amicon ultrafiltration (model 8050) using a YM-30 filter to one-tenth the original volume. The fraction was then either dialyzed for 48 h against 0.5 M NaCl and 10 mM Hepes, pH 7.4, or chromatofocused to purify peripherin/rds as described in detail (*40* and references therein).

Preparation and R_{18} Labeling of ROS Plasma Membranes. ROS disk membrane and plasma membrane vesicles were isolated using ricin-agarose and differential sucrose density gradient centrifugation (*43*). The ROS plasma membrane was eluted from the ricin-agarose using 1 M galactose in 0.1 M sodium borate, pH 8.0. The isolated plasma membrane was washed free of calcium and resuspended in calcium-chelating buffer: 10 mM Hepes and 1.0 mM EGTA, pH 7.2 (*44*). The ROS plasma membranes were labeled with octadecylrhodamine B chloride (R_{18}, Molecular Probes, Inc., Junction City, OR) for 30 min at room temperature in the dark (*18*).

Peripherin/rds recombinants were prepared from purified peripherin/rds isolated from the chromatofocusing procedure. The purified protein was recombined with disk lipid vesicles (from extracted disk lipid membranes) using detergent dialysis (*45*). During the final dialysis step, the recombinant vesicles were dialyzed against SM-2 BioBeads (Bio-Rad). Using this method, less than 0.05 mol % of the OG remained associated with the vesicles. In some experiments, peripherin/rds-enriched Concanavalin-A unbound fractions were dialyzed for 48 h to remove all traces of OG. All vesicle recombinants were subject to five freeze−thaw cycles in liquid N_2 to form large unilammelar vesicles (*24*). The disk lipid vesicles containing no protein were prepared as large unilamellar vesicles (*25*). In preparing the disk lipids used in all of the recombinants, the retinal Schiff-base linkage was reduced using sodium cyanoborohydride, thereby eliminating any retinal-induced membrane fusion due to a lipid-mediated mechanism (*25*).

R_{18} Lipid-Mixing Assay. Fusion assays characterizing R_{18}-labeled plasma membrane−disk membrane fusion were performed exactly as described previously (*18*). R_{18} was incorporated into purified plasma membrane vesicles at self-quenching levels, usually at 3−5 mol % relative to the phospholipid. Upon membrane fusion, R_{18} is diluted throughout the target membrane by lateral diffusion, leading to a dequenching and an increase in fluorescence intensity that is proportional to the membrane fusion (*18*, *24*, *25*, *46*).

Fusion assays using R_{18}-PM and peripherin/rds LUV recombinants or disk membranes were performed and the initial rates of fusion calculated as described (*18*, *46*). In all of the R_{18} lipid-mixing assays, fluorescence and light scattering were measured using a Perkin-Elmer LS-50B spectrofluorometer. Fluorescence was monitored at an excitation wavelength of 560 nm and an emission wavelength of 586 nm. Fusion was initiated with the addition of R_{18}-PM into a suspension of target membranes. The increase in R_{18} fluorescence due to the dilution of the probe in the target membrane was monitored continuously and increased linearly with probe dilution. The fluorescence intensity obtained without the addition of plasma membrane was taken as a baseline. The fluorescence at infinite probe dilution (100% fluorescence) was determined with the addition of 100 μL of 10% Triton X-100 to the membrane mixture. Initial rates of fusion were determined from the increase in fluorescence intensity as a function of time (*46*). The increase in fluorescence was recorded for 10 min. Under these conditions, the increase in fluorescence reached a plateau, and the change in fluorescence over the first 5 min was used to calculate the initial rate of fusion. This assay has been shown to be sensitive to the fusion of disk membranes with PE LUVs and disk lipid vesicles as well as fusion between plasma membrane and disk membranes (*18*, *24*, *25*, *40*).

In some experiments, the disk membranes or peripherin/rds LUVs were pretreated with either antiperipherin monoclonal antibody 2B6 or various peptides for 10 min in the dark at 37 °C. Fusion was initiated with the addition of R_{18}-PM to these suspensions as described above. The synthetic peripherin/rds peptides designated PP-3 to PP-7 correspond to the C-terminal region of peripherin/rds. The aligned amino acid sequence of these peptides is shown in Table 1. Bradykinin (Sigma, St. Louis, MO) was used as a nonspecific control peptide in these studies. All peptides were added in 10 mM Hepes at the concentrations indicated in the figures and tables.

Proteolysis Procedure. Disk membrane or peripherin/rds LUVs were treated with papain as described (*47*). Briefly, samples to be proteolyzed were resuspended in 100 mM NaCl, 10 mM glycine, and 0.1 mM EDTA with 5 mM cysteine, pH 7.2 (buffer was made fresh daily). The samples were incubated for 30 min in the dark with an appropriate volume of papain (stock 25 mg/mL), such that the ratio of papain to total protein was 20:1. The reaction was terminated with the addition of iodoacetamide (final concentration, 10 mM). The papain-treated membranes were washed and resuspended in 10 mM HEPES, pH 7.2.

ROS disk membranes or peripherin/rds LUVs were proteolyzed with trypsin as described previously (*34*). Briefly, samples were incubated with trypsin (final concentration 0.2

μg/mL) for 30 min in the dark at 37 °C. The reaction was stopped with the addition of 4.0 μg of trypsin inhibitor. The trypsin treated samples were washed in 10 mM Hepes, pH 7.2, and centrifuged at 60 000 rpm for 40 min. The pellet was resuspended in 10 mM Hepes, pH 7.2, for fusion assay. The supernatant from purified peripherin/rds recombinants was saved and stored on ice prior to use in the ANTS/DPX contents mixing assay.

The extent of proteolysis (trypsin or papain) was determined using SDS−PAGE as described (*30*). Protein was visualized using silver staining (*48*). The C-terminal region of peripherin/rds was detected with mAb2B6 (*27*) using western blotting as described (*40*).

ANTS/DPX Contents Mixing Assay. Large unilamellar vesicles (LUVs) encapsulating either ANTS or DPX were prepared as described (*49*) and modified (*50*). LUVs were prepared from 95 mol % *N*-methyl-DOPE and 5 mol % PS (bovine brain). These lipids were cosolubilized in chloroform, dried under N_2, and lyophilized to remove trace amounts of chloroform. The dried phospholipids were hydrated either in 25 mM ANTS, 45 mM NaCl, and 10 mM glycine, pH 9.5, or in 90 mM DPX and 10 mM glycine, pH 9.5. All hydrations were done on ice under N_2 for 3 h. The lipid suspension was subject to five freeze−thaw cycles and extruded through a polycarbonate membrane, 0.1 μm pores (Nucleopore Corp, Pleasanton, CA), 10 times. Encapsulated fluorescent probe was separated from free probe on a Sephadex G-50 column (Pharmacia) eluted with 100 mM NaCl, 10 mM glycine, and 0.1 mM EDTA, pH 9.5. Vesicles were stored on ice under N_2 and used within 2 days.

Fluorescence measurements were made on a Perkin-Elmer LS50B spectrofluorometer. The ANTS/DPX fusion assays were carried out as described (*51*). Fluorescence intensity was monitored at $\lambda_{ex} = 380$ nm and $\lambda_{em} = 510$ nm. All fusion assays were carried out in a total volume of 3 mL. In these assays, a 9:1 molar ratio of DPX-containing LUVs to ANTS-containing LUVs was used. The LUVs were allowed to equilibrate to the appropriate temperature for 5 min. $CaCl_2$ (final concentration 67 μM) and various peptides (concentration 70 nM) were added to the LUVs and preincubated prior to the initiation of fusion. The addition of peptide did not change the final pH. Fusion of LUV was initiated by lowering the pH from 9.5 to 4.5 with the addition of 2 M sodium acetate/acetic acid. Fusion of *N*-methyl-DOPE:PS vesicles containing either ANTS or DPX was detected as a decrease in fluorescence intensity as the aqueous contents are mixed and an ANTS−DPX complex is formed. The observed fluorescence quenching is due to the reduced quantum yield of this ANTS−DPX complex. Baseline fluorescence was taken to be the intensity obtained with the shutters closed. Fluorescence at 100% is taken to be the initial fluorescence intensity before lowering the pH. The initial slope of the fluorescence decay curve was used to calculate the initial rate of fusion as described previously (*51*). The initial slopes were determined 30−60 s immediately following the initiation of fusion.

Aggregation Studies. The LUVs used in the turbidity studies were prepared as described above for the ANTS−DPX contents mixing experiments except the phospholipid composition was *N*-methyl-DOPE (75 mol %), PC (egg, 10 mol %), and PS (bovine brain, 15 mol %). The calcium-induced aggregation of LUVs was monitored by following the change in absorbance at 400 nm in a Perkin-Elmer 2.0 UV/VIS spectrometer (*52*). LUVs (final phosphate concentration 1.5 mM) were preincubated with the designated amount of peptide for 10 min at the indicated temperatures. On the basis of a calcium titration curve, it was determined that 16 μM $CaCl_2$ was sufficient to induce aggregation and very little fusion in this system. The absorbance was recorded every 0.1 min for 15 min. Reversible aggregation was distinguished from fusion with the addition of 100 mL of 1 M EDTA, and the absorbance monitored for an additional 3 min.

Fourier Transform Infrared Spectroscopy (FTIR) and Quantitative Estimation of PP-5 Structure. For infrared spectroscopy, lipid vesicles were prepared by dispersing purified bovine disk lipids in 5 mM Hepes buffer prepared in D_2O, pD 7.8, at a concentration of 40 mg/mL. The lipid dispersion was vortexed, sonicated for 5 min, and then lyophilized for 1 h to yield a dry powder. The lyophilized powder was resuspended in the above buffer for 1 h at ambient temperature in a dry N_2 atmosphere. Reconstituted PP-5 peptide samples were prepared by mixing aliquots of pure PP-5 with the solubilized lipid vesicles. The final concentration of peptide in these samples was 2 mg/mL. The reconstituted sample was allowed to stand in a sealed infrared compartment purged with dry N_2 for 25 min. The sample was lyophilized and resuspended in D_2O, and sufficient time was allowed prior to data collection to ensure complete deuteration as monitored by observing amide A (3300 cm^{-1}, N−H stretching and amide II 1550 cm^{-1}, N−H bending) bands. The final concentration of the sample was adjusted to 50 mg/mL. FTIR spectra were collected from at least two sets of experiments to ensure reproducibility.

The samples were placed in sealed IR AgBr window cells spaced by Teflon spacer with a path length of 0.01 mm. The infrared data were acquired at ambient temperatures with a Nicolet (Magna IR-550) FTIR spectrometer equipped with a liquid N_2 cooled DTGS detector and a Ge-coated KBr beam splitter (*53*). All spectra were recorded at a resolution of 2 cm^{-1} by coadding 256 double-sided interferograms which were Fourier transformed after application of a Happ-Genzel apodization function. The spectrometer and sample compartments were continuously purged with dry N_2.

For quantitative estimation of peptide secondary structure, curvefitting analysis was accomplished by decomposition of the original amide I band following an improved procedure (*54*). In brief, after obtaining the optimum number of band positions and estimations of bandwidths by partial Fourier deconvolution and second derivation as described earlier, the iterative process is performed in CURVEFIT running under advanced Grams/32 software (Galactic Industries Corp., Salem, NH) using the height of the amide band as the initial intensity estimation. A voigt line shape function combination of a Gaussian and Lorentzian band shape was assumed to fit the observed band components, and a Bessel apodization function was used. The γ fraction was kept constant at 4 for all band fits for the first 100 iterations. Then, the γ fraction was allowed to change in all the bands and about 100 more iterations performed. The final parameters are used to calculate the percentage of band areas, not taking into account the contributions of side chains between 1624 and 1600 cm^{-1}.

Predicted Model. The prediction of the secondary structure of the peptides was derived on a silicon graphics VGX workstation using a loop search technique with SYBYL. The secondary strucure was predicted according to the method of Robson-Garnier (*55*) and the hydrophilicity plots calculated according to the algorithm of Hopp and Woods (*56*) with the window set to 7.

Additional Assays. Phosphate was determined as described by (*57*) and modified by (*58*). Total protein was determined using a Bio-Rad microassay procedure (Sigma, St. Louis, MO).

RESULTS

Fusion between ROS disk membranes and the surrounding plasma membrane occurs in an in vitro cell-free fusion system and is postulated to be necessary in disk packet formation (*18*). The disk rim specific protein, peripherin/rds, is involved in this fusion process (*40*). Beginning with an in vitro cell-free assay system, utilizing R_{18}-labeled plasma membrane (R_{18}-PM), and disk membranes and advancing to a model system, R_{18}-PM and peripherin/rds LUVs, we have provided compelling evidence for a role of peripherin/rds as a membrane fusion protein. Continuing with experiments using purely model membranes, we have documented the fusogenic nature of the C-terminal region of this protein. Fusion between R_{18}-PM and disk membranes was recorded as a linear increase in R_{18} fluorescence in a lipid mixing assay (Figure 1A). However, when R_{18}-PM fused with peripherin/rds-enriched disk lipid large unilammellar vesicles (LUVs), a lag-phase lasting 120 s, during which time little or no fusion occurred, preceded the linear increase in R_{18} fluorescence, at 37 °C. (Figure 1B). The lag-time increased, to almost 300 s in duration, when the temperature was lowered to 30 °C (Figure 1B).

Viral membrane fusion studies have shown that lag-phases are indicative of the formation of a fusogenic state, suggesting a protein-mediated process (*59*, *60*). To investigate whether the fusion between R_{18}-PM and disk membranes or peripherin/rds LUVs was protein dependent, the target membranes (either disk membranes or peripherin/rds LUVs) were proteolyzed prior to the initiation of fusion. By selectively proteolyzing peripherin/rds versus rhodopsin, we were able to distinguish between the involvement of these two proteins in the fusion response. Trypsin cleaves both peripherin/rds (*34*) and rhodopsin (*61*), whereas only rhodopsin is sensitive to papain proteolysis (*47*).

The initial rate of fusion between R_{18}-PM- and trypsin-treated disk membrane was lower than that observed in controls (Table 2). Similarly, when R_{18}-PM fused with trypsin treated peripherin/rds LUVs, a decrease in the initial rate of fusion and an increase in lag-time were observed (Table 2). Since both rhodopsin and peripherin/rds are membrane proteins, it is expected that the trypsin cleavage products may be recovered in the supernatant from the trypsinolysis experiment. This in fact was the case, a major 12.5 kDa fragment was isolated from the supernatant of peripherin/rds LUVs treated with trypsin. On the basis of Western blot analysis, this fragment was found to be immunoreactive with anti-peripherin/rds, mAb 2B6, and to correspond to the C-terminal region of peripherin/rds (data not shown). The addition of the trypsin supernatant to

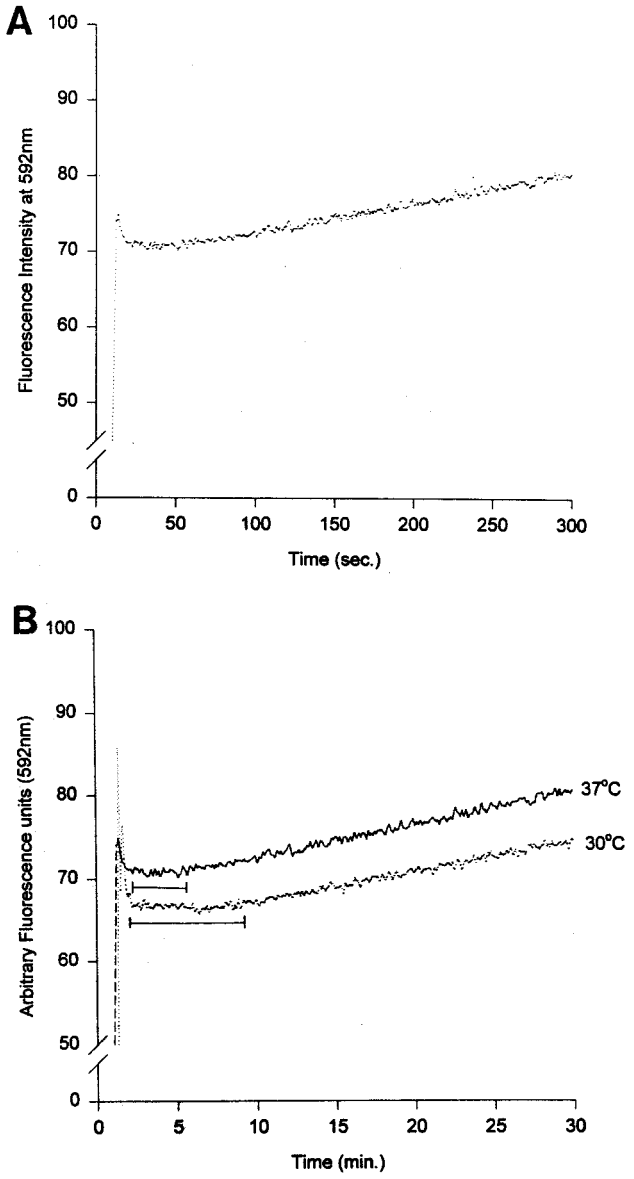

FIGURE 1: (A) Membrane fusion between R_{18}-PM and disk membranes. The increase in fluorescence intensity of R_{18} at 592 nm over time (seconds) upon the addition of R_{18}-PM to disk membranes is shown. Fusion was initiated with the addition of R_{18}-PM at 10 s to unlabeled disk membranes and the increase in fluorescence intensity followed over time at 37 °C. The results are that of a representative experiment. (B) Membrane fusion between R_{18}-PM and peripherin/rds LUVs. The increase in fluorescence intensity of R_{18} at 592 nm over time (minutes) upon the addition of R_{18}-PM (at 15 s) to peripherin/rds disk lipid LUVs is shown at 37 °C, (A) at 30 °C (B). The horizontal solid lines indicate the "lag-times". The results are that of a representative experiment.

trypsin-treated peripherin/rds LUVs restored the fusion in this system (Table 2). The addition of trypsin supernatant, from the trypsinolysis of purified peripherin/rds, to untreated disk membranes (Table 2) or peripherin/rds LUVs (data not shown) enhanced the initial rate of fusion between these membranes and R_{18}-PM. In contrast, papain proteolysis of the disk membrane or peripherin/rds LUVs had no effect on the fusion of these membranes with R_{18}-PM (Table 2). Thus, while rhodopsin is the most abundant protein in the disk membranes, it is most likely not involved in R_{18}-PM disk membrane fusion, since papain proteolysis of rhodopsin had no effect on membrane fusion. This result is confirmed by

Table 2: Effect of Proteolysis on Fusion between R_{18}-PM and Target Membranes[a]

target membrane	additions	lag time (s)	IRF (% ΔFl/s)
LUVs			
peripherin/rds	1 μM Ca^{2+}	120	0.300 ± 0.030
trypsin-treated peripherin/rds	1 μM Ca^{2+}	250	0.150 ± 0.005
trypsin-treated peripherin/rds	1 μM Ca^{2+}, trypsin Sup	30−50	0.25 ± 0.01
peripherin/rds	1 μM Ca^{2+}, trypsin Sup	120−200	0.28 ± 0.02
papain-treated peripherin/rds	1 μM Ca^{2+}	30−40	0.30 ± 0.01
papain-treated peripherin/rds	1 μM Ca^{2+}, papain Sup	30−40	0.33 ± 0.07
disk membranes			
disk membranes	1 μM Ca^{2+}	20−30	0.29 ± 0.04
trypsin-treated disk membranes	1 μM Ca^{2+}	20−40	0.18 ± 0.01
papain-treated disk membranes	1 μM Ca^{2+}	20−40	0.21 ± 0.02
disk membranes	1 μM Ca^{2+}, trypsin Sup	80−120	0.340 ± 0.005

[a] Membrane fusion was measured as an increase in R_{18} fluorescence intensity upon the addition of R_{18}-PM to the unlabeled LUVs or disk membrane preparations (at a final phospholipid concentration of 1 μM). All fusion assays were performed at 37 °C. The trypsin supernatants (trypsin Sup) or papain supernatants (papain Sup) were prepared as described in detail in the Experimental Procedures. The samples were preincubated with the indicated supernatants for the times indicated in the Experimental Procedures, at 37 °C. The initial rates of fusion (IRF) are calculated as the percent change in maximal fluorescence intensity/second. Each value is reported as the mean initial rate of fusion and standard deviation of at least three independent assays.

previous studies in which we have shown that rhodopsin disk lipid vesicle recombinants were unable to fuse with R_{18}-PM under any of the conditions studied (*40*).

The temperature dependence of the fusion between R_{18}-labeled plasma membrane and peripherin/rds LUVs is shown in Figure 2. The initial rate of fusion between these membrane species increased as a function of increasing temperature, with the highest rates of fusion observed at 37 °C. Fusion could not be detected in this system at temperatures higher than 42° C (data not shown). These results are consistent with previous studies in which disk membranes were shown to fuse with model membranes in a temperature-dependent manner (*24*).

Since the inhibitory effect of peripherin/rds trypsinolysis on fusion could be restored with the addition of trypsin supernatant (Table 2), we reasoned that peptide factors in the supernatant enhance membrane fusion. To clearly distinguish between the effects of peripherin/rds peptides and trypsin itself on membrane fusion, we needed to use a membrane system containing no protein components. In addition, because it is difficult to evaluate how the trypsin cleavage products enhance fusion using complex biological membranes, we turned to a model membrane system in which the mechanism by which fusion occurs could be clearly evaluated. Utilizing the ANTS/DPX vesicle contents mixing assay, we were able to evaluate the effect of trypsin cleaved peripherin/rds peptides on membrane fusion. The fusogenic activity of peptide factors in the trypsin supernatant was followed as a decrease in fluorescence upon contents mixing (*50*). The initial rate of contents mixing between

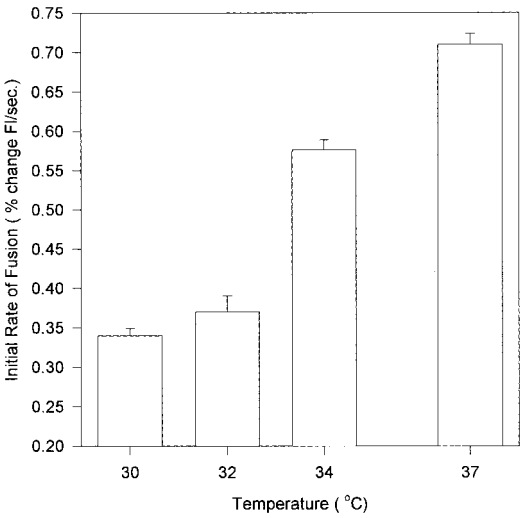

FIGURE 2: Temperature dependence of fusion between R_{18}-PM and peripherin/rds LUVs. The initial rate of fusion between R_{18}-PM and peripherin/rds LUVs is shown as a function of increasing temperature. R_{18} lipid mixing assays were carried out as described in the Experimental Procedures, and the initial rates of fusion are calculated as the change in maximal fluorescence intensity per second. Each value is reported as the mean initial rate of fusion and standard error of the mean of two independent preparations, each assayed in triplicate, for an $n = 6$.

ANTS containing *N*-monomethyl-DOPE:PS (95:5) vesicles and DPX containing *N*-monomethyl-DOPE:PS (95:5) vesicles and vesicles preincubated with trypsin supernatant (with a final peptide concentration of 0.780 nM) was followed for 10 min. All assays contained 6.7 mM calcium, which was added to the vesicles prior to preincubation with trypsin supernatant. In the presence of trypsin supernatant, at 37 °C, an increase in contents mixing from 9.23 ± 1.54 to 31.22 ± 4.62 was observed in control and trypsin supernatant treated vesicles, respectively. Interestingly, contents mixing was increased substantially at 37 and 40 °C (from 15.6 ± 3.5 to 75.3 ± 16.3 in control and trypsin supernatant treated vesicles respectively), further suggesting a protein-mediated process. Each of the values is reported as the mean initial rate of fusion and standard error of the mean of two independent preparations with each assay performed in triplicate, for an $n = 6$. Trypsin itself and trypsin inhibitor had no effect on contents mixing in this system (data not shown), thereby excluding a role for these factors in restoring fusion between R_{18}-PM and trypsin treated target membranes.

C-Terminal Peripherin/rds Peptides Modulate Fusion between R_{18}-PM and Target Membranes. We have previously shown that fusion between R_{18}-PM and peripherin/rds LUVs could be inhibited by anti-peripherin/rds mAb 2B6 (*40*). In the experiments described above, we have documented that trypsinolysis of the C-terminal region of peripherin/rds inhibits membrane fusion. In addition, the trypsin supernatant contained a major peptide fragment, immunoreactive with mAb 2B6 [mAb 2B6 recognizes the tail of the C-terminal region of peripherin/rds (*27*)] that enhanced contents mixing (indicative of membrane fusion). To confirm that the C-terminal of peripherin/rds was involved in fusion between R_{18}-PM and disk membranes, we tested the effects of synthetic peptides, corresponding to regions of the C-terminus, an N-terminal peptide (NP-1) and a peptide to the first intradiskal loop of peripherin/rds (PP-2) on fusion.

Table 3: The Effect of Synthetic Peripherin/rds Peptides on Fusion between R_{18}-PM and Target Membranes[a]

target membrane	additions	lag-time (s)	IRF (% ΔFl/s)
disk membranes	1 μM Ca^{2+}	15	0.75 ± 0.053
	PP-5, 1 μM Ca^{2+}	60	0.371 ± 0.018
	NP-1, 1 μM Ca^{2+}	20	0.71 ± 0.023
peripherin/rds LUVs	1 μM Ca^{2+}	110	0.534 ± 0.009
	NP-1, 1 μM Ca^{2+}	90	0.550 ± 0.087
	PP-2, 1 μM Ca^{2+}	90	0.542 ± 0.053
	PP-7, 1 μM Ca^{2+}	90	0.490 ± 0.012

[a]Membrane fusion was measured as an increase in R_{18} fluorescence intensity upon the addition of R_{18}-PM to the unlabeled LUVs or disk membrane preparations (at a final phospholipid concentration of 1 μM). Samples (either disk membranes or peripherin/rds LUVs) were preincubated (at 37 °C) with the indicated peptides as described in detail in the Experimental Procedures. All fusion assays were performed at 37 °C. The IRFs are calculated as the percent change in maximal fluorescence intensity/second. Each value is reported as the mean initial rate of fusion and standard deviation of at least three independent assays.

Table 4: The Effect of PP-5 Concentration on Fusion between R_{18}-PM and Peripherin/rds LUVs[a]

target membrane	peptide: peripherin/rds (mol:mol)	PL:peptide (mol:mol)	change in lag time	% change in IRF
peripherin/ rds LUVs	4:1	22:1	decrease in lag time by 50 s	25% increase
	1.7:1	55:1	no change	10% increase
	0.5:1	168:1	increase in lag-time by 30 s	7.8% decrease

[a]Membrane fusion was measured as an increase in R_{18} fluorescence intensity upon the addition of R_{18}-PM to the unlabeled LUVS at a final phospholipid concentration of 1 μM. The peripherin/rds LUVs were preincubated with PP-5 at the indicated concentrations, at 37 °C. All fusion assays were performed at 37 °C. The IRFs are calculated as the percent change in maximal fluorescence intensity/second. Peptide: peripherin/rds refers to the ratio of peptide monomers to peripherin/rds monomers (mol:mol) in the fusion assay. PL:peptide refers to the phospholipid to peptide (mol:mol) ratio of the preincubated peripherin/rds LUVs.

As seen in Table 3, preincubation of disk membranes with the C-terminal peptide, PP-5, resulted in an increase in the lag-time and a decrease in the initial rate of fusion between disks and R_{18}-PM, while PP-2 had no effect on this fusion. Preincubation of disk membranes with NP-1, had no effect on the lag-time or on the initial rate of fusion between disk membranes and R_{18}-PM (Table 3). When the disk membranes were preincubated with bradykinin as a nonspecific control peptide, no change in fusion kinetics was observed (data not shown). These studies suggest that the C-terminal region of peripherin/rds is involved in fusion between R_{18}-PM and disk membranes.

To elucidate the mechanism by which the C-terminal region of peripherin/rds may be involved in this fusion process, we investigated the effect these same peptides had on R_{18}-PM−peripherin/rds LUV fusion. When the peripherin/rds LUVs were preincubated with PP-5, an increase in the initial rate of fusion between these LUVs and R_{18}-PM was observed at high peptide concentrations (Table 4). In contrast, a decrease in the initial rate of fusion and an increase in lag time was observed at low peptide concentrations (Table 4). When the peripherin/rds LUVs were preincubated with NP-1 and allowed to fuse with R_{18}-PM, no change in lag-time or initial rate of fusion was observed (Table 3). PP-2, a peptide to the first intradiskal loop of peripherin/rds had no effect on fusion (*40*). Again, preincubation of peripherin/rds LUVs with bradykinin had no effect on the fusion between these LUVs and R_{18}-PM (data not shown).

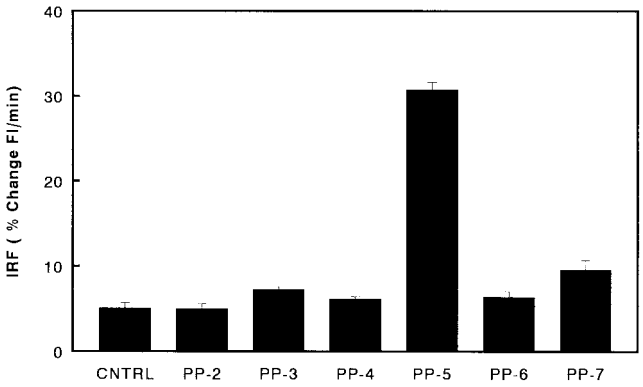

FIGURE 3: Effect of synthetic C-terminal peripherin/rds peptides on ANTS/DPX contents mixing. ANTS containing N-monomethyl DOPE:PS (95:5) vesicles and DPX containing *N*-monomethyl-DOPE:PS (95:5) vesicles were preincubated with the indicated synthetic peptides to the C-terminal region of peripherin/rds at 37 °C for 30 min prior to the initiation of fusion. The final peptide concentration in all of the assays was 10 nM. All assays contained 6.7 mM calcium, which was added to the vesicles prior to preincubation with peptide. Contents mixing was initiated with a drop in sample pH as described in the Experimental Procedures. The addition of peptide had no effect on the initial pH of the samples. Each value is reported as the mean initial rate of fusion and standard error of the mean of three independent preparations with each assay performed in triplicate, for an $n = 9$.

C-Terminal Peripherin/rds Peptides Enhance Contents Mixing and Promote Vesicle Aggregation. Since fusion between peripherin/rds LUVS and R_{18}-PM could be inhibited with anti-peripherin/rds mAb 2B6 (*40*), we investigated the portion of the C-terminal of peripherin/rds known to bind this antibody (*27*). The induction of vesicle contents mixing by various overlapping synthetic C-terminal peripherin/rds peptides was followed to identify the region necessary to facilitate membrane fusion. ANTS−DPX contents mixing was measured using *N*-monomethyl-DOPE:PS (95:5; mol:mol) LUVs in the presence of peptide, at various temperatures. As seen in Figure 3, two peptides, PP-5 and PP-7, enhanced contents mixing, thereby inducing membrane fusion in this vesicle system. The other peptides, PP-2, PP-3, PP-4, PP-6, and bradykinin (data not shown), had no detectable effect on contents mixing.

Biological fusion is a complex phenomenon that involves a series of biochemical and biophysical interactions. Fusion in model membrane systems has been characterized as requiring the following sequence of steps: (1) close approach of two membranes, (2) membrane adhesion, and (3) bilayer destabilization, prior to the actual fusion and mixing of aqueous and lipid contents (*62*). Since the fusogenic properties of PP-5 may be due to an ability to induce membrane aggregation, we investigated whether the various C-terminal peripherin/rds peptides modulated Ca^{2+}-dependent vesicle aggregation, followed as a change in vesicle absorbance at 400 nm. As seen in Figure 4, PP-5, the same peptide that facilitated contents mixing between model membranes also enhanced Ca^{2+}-dependent vesicle aggregation when compared to controls. PP-5 was unable to enhance vesicle aggregation in the absence of calcium (data not shown) or in the presence of another divalent cation Mg^{2+}

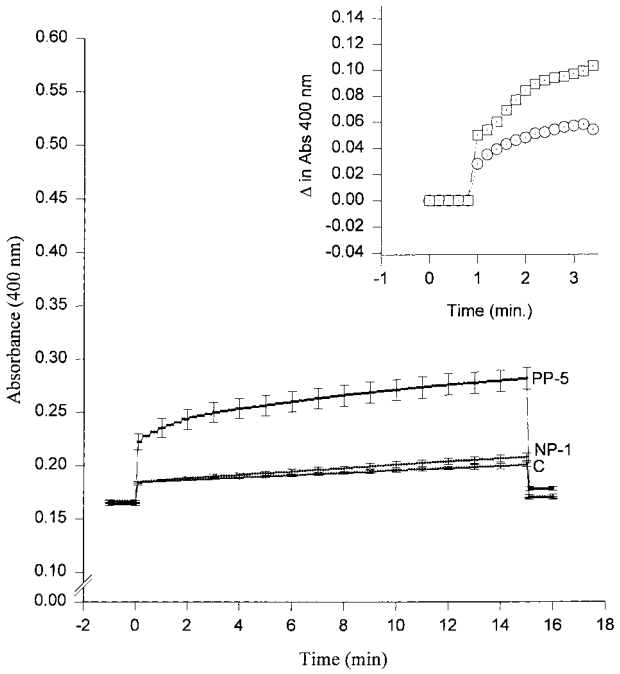

FIGURE 4: Comparison of the effect of PP-5 and NP-1 on calcium-induced vesicle aggregation. The change in absorbance at 400 nm of *N*-monomethyl-DOPE:PC:PS (75:10:15) vesicles in the presence of 1 nM PP 5 (□), 1 nM PP-2 (●) or in the absence of peptide (▲), was monitored over time at 37 °C, as described in the Experimental Procedures. The final calcium concentration in these experiments was 9 mM. Each value is reported as the mean of the absorbance at 400 nm and standard error of the mean of three independent preparations with each assay performed in triplicate, for an $n = 9$. (Inset) Effect of PP-5 on calcium-induced vesicle aggregation. The initial change in absorbance at 400 nm of *N*-monomethyl-DOPE: PC:PS (75:10:15) vesicles in the presence of 1 nM PP-5 (□) or in the absence of peptide (○) was monitored over time at 37 °C, as described in the Experimental Procedures. The final calcium concentration in these experiments was 50 μM. The results are of a representative experiment with each data point representing a single measurement.

(data not shown). In addition, PP-5-enhanced aggregation was increased as the temperature was raised from 15 to 37 °C (data not shown). Interestingly, NP-1-enhanced vesicle aggregation, albeit to a lesser extent than PP-5 (Figure 4). However, NP-1 had no detectable effect on R_{18}-PM fusion with disk membranes or with peripherin/rds LUVs (Table 3). PP-3, PP-4, PP-6, PP-7, and bradykinin had no effect on vesicle aggregation in this system (data not shown).

Biochemical and Predicted Structural Characteristics of C-Terminal Synthetic Peptides. White (*2*) has provided a comprehensive analysis of the biochemical characteristics exhibited by a majority of fusion proteins. To access peripherin/rds as a fusion protein based on biochemical homology with other such proteins, we analyzed the various C-terminal peptides with regard to predicted structure and hydropathic index. The hydropathic index was determined as described in the Experimental Procedures. An algorithmic average of the individual hydropathic indices of the amino acids and their relative relationship to each other was used to predict the structure of the peptides (*55*, *56*). The amphiphilic nature of an α-helix was determined by a calculation of the hydrophobic moment, a value which represents the hydrophobicity of a peptide measured for different angles of rotation (100° for α-helix, 160° for β-structures) per residue. The results of this analysis are shown in Table 5. Two peptides, PP-3 and PP-4, were predicted to form β-conformations by computer algorithms. Neither of these peptides had any effect on ANTS/DPX contents mixing or vesicle aggregation. The most potent fusion peptide was PP-5, a peptide which is shown to be mostly α-helical. This peptide has the lowest hydropathy index, at 0.75 and a hydrophobic moment (μH) of 0.59, suggesting that it most likely forms an amphiphilic structure. Although PP-6 has a similar structural prediction, α-helix and β-turn, this peptide had no fusogenic effect; this may be due to the large hydropathic index of this peptide, at 3.16.

Table 5: Biochemical and Structural Characteristics of Synthetic Peripherin/rds Peptides[a]

peptide	hydropathy index	predicted structure
PP-2	−6.76	α-helix
PP-3	1.79	β-turn
PP-4	6.47	β-turn
PP-5	0.75	α-helix
PP-6	3.16	α-helix
PP-7	2.23	ND
NP-1	−4.03	α-helix

[a] The structure of the synthetic C-terminal peripherin/rds peptides was predicted as described in the Experimental Procedures. The hydropathy index is a measure of free energy needed to transfer a specific amino acid residue to water and is expressed in kilocalories per mole. An algorithmic average of all of the amino acid residues in each peptide and their relative relationship to each other determines the hydropathic index of the peptides and the predicted structure (*53*, *54*). The structure of the five amino acid peptide, PP-7 was not determined, and this is indicated as ND.

To confirm the structural prediction provided by SYBYL, the structure of PP-5 was evaluated using FTIR spectroscopy. FTIR spectroscopy is widely used as a structural tool which provides useful information on conformational properties of peptides. The FTIR spectrum of PP-5 (Figure 5A) in aqueous buffer shows two major peaks located at 1652 and 1674 cm^{-1} indicative of a largely α-helical and β-bend conformation, respectively (*54*, *63*). When the structure of the peptide is analyzed in the presence of disk lipid liposomes (Figure 5B), there is a slight shift in the amide I region from 1652 to 1643 cm^{-1}; such a shift with a small peptide is consistent with a distorted helical conformation and may be consistent with a peptide−lipid interaction (6). When PP-5 is modeled as an α-helical structure, the amphipathic nature of this peptide becomes apparent (Figure 6).

DISCUSSION

Collectively, the data presented provide compelling evidence identifying peripherin/rds as the first fusion protein in photoreceptor rod cells. Evidence supporting this hypothesis include (1) the inhibition of R_{18}-PM disk membrane fusion by trypsinolysis of peripherin/rds and by preincubation of disk membranes with peripherin/rds monoclonal antibody (mAb 2B6) and by synthetic peptides to the C-terminal region of peripherin/rds, (2) the initiation of fusion between R_{18}-PM and disk lipid vesicle recombinants containing purified peripherin/rds, (3) the inhibition of fusion between R_{18}-PM and peripherin/rds LUVs in the presence of synthetic C-terminal peripherin/ rds peptides, (4) the identification of a putative fusion peptide designated, PP-5, within the C-terminal region of peripherin/rds, which promotes aqueous contents mixing and vesicle aggregation. Since cone shed-

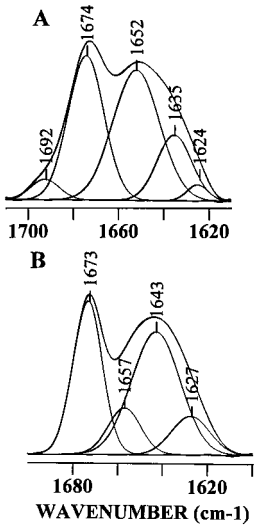

FIGURE 5: FTIR spectra of thin films of PP-5. The amide I′ region of the peripherin/rds peptide PP-5, after partial Fourier self-deconvolution obtained in 5 mM deuterated spectra in Hepes buffer, pD 7.8, is shown without disk liposomes (A) and in the presence of disk liposomes (B). FTIR spectroscopy was carried out and the data analyzed as described in detail in the Experimental Procedures. The concentration of the disk lipid liposomes was 40 mg/mL phospholipid. The two peaks at 1624 and 1692 cm^{-1} are not the amide I′ components, though they constitute about 2−4%, respectively, of the secondary structure and are excluded from the structural analysis.

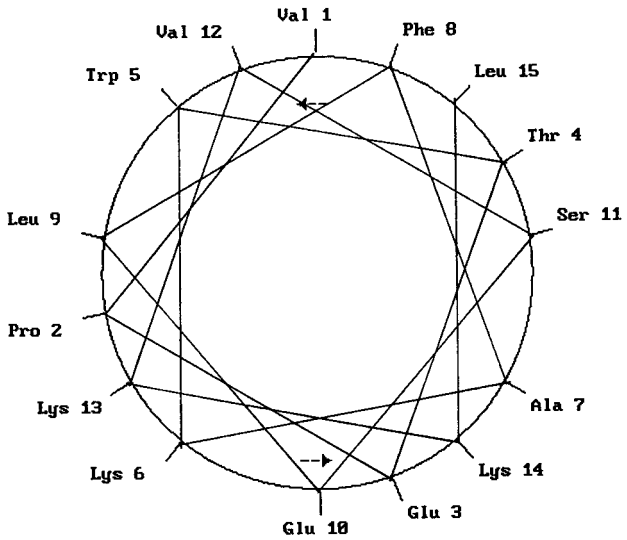

FIGURE 6: Schematic representation of the α-helical wheel of PP-5 corresponding to residues 311−325. On the basis of the structural parameters inferred form SYBYL and the FTIR spectra, the amphiphilic α-helical structure of peripherin/rds can be modeled as shown. The α-helix was drawn with the aid of Helwheel software. The position of the individual amino acids is given by the numbers next to the various residues.

ding also involves the fusion of an evaginated peripherin/rds-enriched rim region with the surrounding plasma membrane, peripherin/rds may also be a candidate fusion protein in cones cells as well.

Proteins implicated in targeted membrane fusion are postulated to aid in the thermodynamically unfavorable fusion event by promoting hydrophobic interactions that favor fusion. Most fusion proteins are membrane anchored, as is peripherin/rds (*27*, *29*) and products of a single gene, as is peripherin/rds (*26*). The function of these membrane proteins is imparted by the presence of fusogenic regions or patches of amino acids within their N-terminal or, in some cases, C-terminal domains. White (*2*) has provided a comprehensive analysis of the biochemical characteristics of such fusion peptides. These peptides are usually short stretches of relatively hydrophobic amino acids (16−25 residues) within membrane-anchored domains and may be internal to the polypeptide chain (*2*). They have a hydrophobicity index between 0.50 and 0.70, and when modeled as α-helices, they display one face with a high hydrophobicity index and a back face that has hydrogen-bonding potential. Utilizing a series of synthetic peptides corresponding to overlapping regions between residues 308 and 345 of the C-terminal of peripherin/rds, we have identified a fusogenic region of amino acids, from residue 313 to 327 (designated as peptide PP-5 in Table 1), which was shown to promote membrane fusion in vitro. Since other peptides within this series of overlapping peptides had no effect on either R_{18}-PM disk membrane or peripherin/rds LUV fusion or model membrane fusion, it appears that the sequence corresponding to PP-5 is sufficient to modulate fusion. PP-5 is a short 16 amino acid long peptide, predicted to be α-helical (Table 5). FTIR spectroscopy confirmed this conformation (Figure 5A). When modeled as an α-helix (Figure 6), it is amphiphilic, a characteristic consistent with its role as a fusogenic region. In the experiments presented herein, this peptide enhances model membrane fusion and stimulates vesicle aggregation. What role, if any, the remainder of the C-terminus plays in peripherin/rds interactions with the plasma membrane remains to be determined.

We have previously shown that peripherin/rds is phosphorylated on a C-terminal serine residue (*40*). Given that phosphorylation of peripherin/rds enhances membrane fusion (*40*), it is tempting to speculate that ser_{321} (located within the fusogenic patch) is phosphorylated and contributes to the overall fusogenic nature of this region of the protein. Studies are presently underway to identify the site of phosphorylation and role of phosphoperipherin/rds in fusion.

Peripherin/rds is somewhat unique in that both the C-terminal region and the N-terminal region may contribute to the fusion process. Data supporting a role for the N-terminus include only a 30% decrease in disk-PM fusion upon trypsinolysis. On the basis of the sequence of peripherin/rds, both the C-terminal region and N-terminal region may be cleaved by trypsin. The role of the N-terminus is unclear since an N-terminal peptide, NP-1, enhances membrane adhesion but had no effect on fusion between PM and disk or peripherin/rds LUVs. The simplest interpretation of these results is that this region is not involved in a rate-limiting step of the process. However, the ability, in part, of the trypsin supernatant, to promote fusion may be due to the N-terminal region promoting membrane adhesion

Fusion between ROS disk membranes and R_{18}-PM is a calcium-dependent process (*18*). The experiments presented confirm this observation and show that fusion between R_{18}-PM and peripherin/rds LUVs also requires submicromolar levels of calcium. The reason for the necessity of calcium has now become apparent. On the basis of the vesicle aggregation studies presented herein, calcium appears to be required for peripherin/rds-promoted vesicle aggregation through PP-5. This interpretation is consistent with previous

studies in which we have shown that magnesium is unable to substitute for calcium in the fusion between R_{18}-PM and disk and in this series of studies in which we have shown that magnesium is unable to induce PP-5 enhanced vesicle aggregation (*18*, *40*, present data).

Fusion of R_{18}-PM with peripherin/rds LUVs has associated with it a distinctive "lag-phase". Others have suggested (*1*, *2*, *59*) that during this time a regulatory step (i.e., formation of a fusion competent state) occurs and a similar process may be occurring here. The formation of such a fusion-competent state may be inferred from the data in Figure 1 (appearance of a temperature and protein dependent lag-time) and Table 4, showing the effect of PP-5 on R_{18}-PM−peripherin/rds LUV fusion. The reciprocal relationship between the ability of PP-5 to increase lag-time and to increase the initial rate of fusion suggests that an additional requirement is necessary for fusion to occur between plasma membrane and peripherin/rds LUVs. This requirement may be the binding of peripherin/rds to a specific site on the plasma membrane surface and/or a change in peripherin/rds conformation upon membrane association. Such a change in conformation is seen in the data presented in Figure 5B, from an α-helical to a somewhat distorted α-helical structure upon membrane association. These results are consistent with the notion that this region of peripherin/rds represents a binding site. Similar requirements have been documented for HIV fusion processes (*64*). When the data in Table 4 are analyzed, taking into consideration the formation of peripherin/rds oligomers in the LUVs, it becomes apparent that at peptide:peripherin/rds tetramer ratios of 1:1, an increase in fusion and decrease in lag-time is observed. In contrast, when the peptide is less concentrated (i.e., at peptide:peripherin/rds homotetramer ratios of 0.4:1.0 and 0.135:1.0), an increase in the lag-time of the fusion process is observed. These results indirectly suggest that four peptides may interact to provide a fusion-competent conformation. Given, that the peptides tested in these experiments were not anchored to the membrane (as is the case with native peripherin/rds), the stoichiometry of peripherin/rds necessary for fusion is speculative.

Peripherin/rds' role as a membrane fusion protein is also consistent with clinical phenotypes of peripherin/rds mutations. Mutations in peripherin/rds are associated with a variety of visual defects (for review see refs *65*−*67*) including retinal degenerations, retinitis pigmentosa, and macular degeneration. In an animal model of retinal degeneration, the *rds* mouse, the peripherin/rds gene is defective (*68*). The ROSs of these *rds* mouse homozygotes do not develop, and the photoreceptor cells eventually die (*27*−*29*, *69*). Interestingly, in adult heterozygotes, the rod outer segments are reduced in length and appear morphologically abnormal (*31*, *32*). These abnormalities begin at approximately 2 months of age and progress throughout life, eventually resulting in cell degeneration and blindness (*31*, *32*). The retinal phenotype of the *rds* heterozygote (*31*, *32*) provides clinically based evidence for the role of peripherin/rds in membrane fusion. These mice exhibit increases in the size and number of phagosomes, suggesting the involvement of normal peripherin/rds in the shedding process. Unregulated fusion between rds/+ mice disk membranes and plasma membrane is likely to contribute to this phenomenon.

In vivo, peripherin/rds exists as a heterotetrameric complex with a nonglycosylated homologue, rom-1 (*35*, *37*, *68*−*70*). To date, no mutations in rom-1 have been associated with retinal degenerations; only digenic mutations with peripherin/rds have resulted in clinical phenotypes (*71*, *72*). The simplest interpretation of these studies is that rom-1 may not be essential for peripherin/rds-induced membrane fusion, although it may be necessary for disk rim formation. Although peripherin/rds and rom-1 share substantial sequence homology, this homology does not occur within the fusogenic C-terminal region (*35*). The contribution of rom-1 to membrane fusion in this system needs to be evaluated utilizing a purified native rom-1 recombinant system as described previously for peripherin/rds (*40*).

Bovine peripherin/rds shares greater than 90% identity with other mammalian peripherin/rds and a 70% homology with *Xenopus* rds [xrds (*73*)]. We compared the homology between bovine peripherin/rds, mouse peripherin/rds, and *Xenopus* peripherin/rds (*73*) and found that, within the fusogenic PP-5 peptide region, there are six conserved residues corresponding to positions 311, 313, 314, 320, 323, and 325. In a comparison of bovine and mouse peripherin/rds, only amino acid 322 is varied from a valine to a phenylalanine in the mouse rds (*73*). This single substitution does not substantially alter the hydropathy index of the fusogenic peptide. Interestingly, phylogenetic homology is seen between amino acids 294−314, a region containing a portion of PP-5 (*73*). Thus, this region of peripherin/rds may be necessary in the newly described functional role of peripherin/rds as a membrane fusion protein.

Biological and viral membrane fusion processes are mediated by either a variety of protein cofactors or both lipid and protein components. Clearly, the process by which peripherin/rds mediates membrane fusion is a complex phenomena. The data presented herein raise interesting questions in regards to what other factors may be necessary for fusion and what triggers fusion in this system. Interactions between the different regions of peripherin/rds may play a regulatory role in the formation of a fusion-competent state. The role of the extradiskal loop and N-terminal region of peripherin/rds in mediating fusion clearly needs to be determined, and experiments are presently underway to identity the respective roles these regions of the protein play in ROS fusion processes.

ACKNOWLEDGMENT

We are grateful to Dr. Robert Molday for the generous gifts of peripherin/rds monoclonal antibody, 2B6, and rom-1 monoclonal antibody, 1D5. The authors would also like to thank Dr. Richard Schimmel for his critical reading of the manuscript and helpful suggestions and Dr. Subhasis Biswas for his assistance with the α-helical models.

REFERENCES

1. Hernandez, L. D., Hoffman, L. R., Wolfsberg, T. G., and J. M. White (1996) *Annu. Rev. Cell Dev. Biol. 12*, 627−661.
2. White, J. (1992) *Science 258*, 917−924.
3. Muga, A., Neugebauer, W., Hirama, T., and Surewicz, W. T. (1994) *Biochemistry 33*, 4444−4448.
4. Takahashi, S. (1990) *Biochemistry 29*, 6257−6264.
5. Harter, C., James, P., Bachi, T., Semenza, G., and Brunner., J. (1989) *J. Biol. Chem. 264*, 6459−6464.

6. Brasseur, R., Vandenbranden, M., Cornet, B., Burny, A., and Ruysschaert, J. M. (1990) *Biochim. Biophys. Acta 1029*, 267−273.
7. Horth, M., Lambrecht, B., Chuah, M., Khim, L., Bex, F., Thiriart, C., Ruysschaert, J.-M., Burny, A., and Brasseur, R. (1991) *EMBO J. 10*, 2747−2755.
8. Stegmann, T., Doms, R. W., and Helenius, A. (1989) *Annu. Rev. Biophys. Biophys. Chem. 18*, 187−211.
9. Tsurudome, M., Gluck, R., Graf, R., Falchetto, R., Schaller, U., and Brunner, J. (1992) *J. Biol. Chem. 267*, 20225−20232.
10. Pak, C. C., Krumbiegel, M., Blumenthal, R., and Raviv, Y. (1994) *J. Biol. Chem. 269*, 14614−14619.
11. Ruigrok, R. W., Aitkin, A., Calder, L. J., Martin, S. R., Skehel, J. J., Wharton, S. A., Weis, W., and Wiley, D. C. (1988) *J. Gen. Virol. 69*, 2785−2795.
12. Wharton, S. A., Martin, S. R., Ruigrok, R. W., Skehel, J. J., and Wiley, D. C. (1988) *J. Gen. Virol. 69*, 1847−1857.
13. Stegmann, T., Bartoldus, I., and Zumbrum, J. (1995) *Biochemistry 34*, 1825−1832.
14. Hughson, F. M. (1995) *Curr. Biol. 5*, 265−274.
15. Guy, H. R., Durell, S. R., Schoch, C., and Blumenthal, R. (1992) *Biophys. J. 62*, 95−97.
16. Stryer, L. (1986) *Annu. Rev. Neurosci. 9*, 87−95.
17. Steinberg, R. H., Fisher, S. K., and D. H. Anderson (1980) *J. Comput. Neurol. 190*, 501−518.
18. Boesze-Battaglia, K., Albert, A. D., and Yeagle, P. L. (1992) *Biochemistry 31*, 3733−3737.
19. Young, R. W. (1976) *Invest. Ophthalmol. Vis. Sci. 15*, 700−710.
20. Corless J. M., and Costello, M. J. (1981) *Exp. Eye Res. 32*, 217−228.
21. Tsukamoto, Y., and Yamada, Y. (1982) *Exp. Eye Res. 34*, 675−694.
22. Laties, A. M., Bok, D., and Liebman, P. (1976) *Exp. Eye Res. 23*, 139−148.
23. Matsumoto, B., and Besharse, J. C. (1985) *Invest Ophthamol. Vis. Sci 26*, 628−635.
24. Boesze-Battaglia, K., and Yeagle, P. L. (1992) *Invest Ophthalmol. Vis. Sci. 33*, 484−493.
25. Boesze-Battaglia, K., Fliesler, S. J., Jun, L., Young, J. E., and Yeagle, P. L. (1992) *Biochim. Biophysc. Acta 1111*, 256−262.
26. Travis, G. H., Brennan, M. B., Danielson, P. E., Kozak, C. A., and Sutcliffe, J. G. (1989) *Nature 338*, 70−73.
27. Connell, G., and Molday, R. S. (1990) *Biochemistry 29*, 4691−4698.
28. Usukura, J., and Bok, D. (1987) *Exp. Eye Res. 45*, 501−515.
29. Jansen, H. G., and Sanyal, S. (1984) *J. Comput. Neurol. 224*, 71−84.
30. Travis, G. H., Sutcliffe, J. G., and Bok, D. (1991) *Neuron 6*, 61−70.
31. Hawkins, R. K., Jansen, H. G., and Sanyal, S. (1985) *Exp. Eye Res. 41*, 701−720.
32. Sanyal, S., and Hawkins, R. K. (1988) *Vision Res. 28*, 1171−1178.
33. Arikawa, K., Molday, L., Molday, R. S., and Williams, D. S. (1992) *J. Cell. Biol. 116*, 659−667.
34. Molday, R. S., Hicks, D., and Molday, L. (1987) *Invest Ophthamol. Vis. Sci. 28*, 50−56.
35. Bascom, R. A., Manara, S., Collins, L., Molday, R. S., Kainins, V. L., and McInnes, R. R. (1992) *Neuron 8*, 1171−1184.
36. Moritz, 0. L., and Molday, R. S. (1996) *Invest. Ophthalmol. Vis. Sci. 37*, 352−362.
37. Goldberg, A. F. X., Moritz, L., and Molday, R. S. (1995) *Biochemistry 34*, 14213−14219.
38. Goldberg, A. F. X., and Molday, R. S. (1996) *Biochemistry 35*, 6144−6149.
39. Goldberg, A. F. X., and Molday, R. S. (1996) *Proc. Natl. Acad. Sci. U.S.A. 93*, 13726−13730.
40. Boesze-Battaglia, K., Kong, F., Lamba, O. P., Stefano, F. P., and Williams, D. S. (1997) *Biochemistry 22*, 6835−6846.
41. Smith, H. G., Stubbs, G. W., and Litman, B. J. (1975) *Exp. Eye Res. 20*, 211−219.
42. Litman, B. J. (1982) *Methods Enzymol. 81*, 150−153.
43. Boesze-Battaglia, K., and Albert, A. D. (1989) *Exp. Eye Res. 49*, 699−701.
44. Robertson, S., and Potter, J. (1984) *J. Pharmacol. 5*, 63−75.
45. Wilson, M. J., Richter-Lowney, K., and Daleke, D. (1993) *Biochemistry 32*, 11302−11307.
46. Hoekstra, D, Boer, T. D., Klappe, K., and Wilschut, J. (1984) *Biochemistry 23*, 5675−5681.
47. Albert, A. D., and Litman, B. J. (1978) *Biochemistry 17*, 3893−3898.
48. Merril, C. R., Goldman, D., and Van Keuran, M. L. (1982) *Electrophoresis 3*, 17−25.
49. Szoka, F., Olson, F., Heath, T., Vail, W., Mayhew, E., and Papahadjopoulos, D. (1980) *Biochim. Biophys. Acta 601*, 559−571.
50. Ellens, H., Bentz, J., and Szoka, F. C. (1985) *Biochemistry 24*, 3099−3106.
51. Kelsey, D., Flanagan, T, Young, J. E., and Yeagle, P. L. (1991) *Virology 182*, 690−702.
52. Kliger, Y., Aharon, A., Rapaport, D., Jones, P., Blumenthal, R., and Shai, Y. (1997) *J. Biol. Chem. 272*, 13496−13505.
53. Lamba, O. P., Borchman, D., and Garner, W. H. (1993) *Exp. Eye Res. 57*, 1−12.
54. Lamba, O. P., Borchman, D., Sinha, S. K., Shah, J., Renugopalakrishnan, V., and Yappert, M. C. (1993) *Biochim. Biophysc. Acta 1163*, 113−123.
55. Garnier, J., Osguthorpe, D. J., and Robson, B. (1978) *J. Mol. Biol. 120*, 97−102.
56. Hopp, T. P., and Woods, K. R. (1981) *Proc. Natl. Acad. Sci. U.S.A. 78*, 3824−3828.
57. Bartlett, G. R. (1959) *J. Biol. Chem. 234*, 466−473.
58. Litman, B. J. (1973) *Biochemistry 13*, 2545−2554.
59. Emans, N., and Verkman, A. S. (1996) *Biophys. J. 71*, 487−494.
60. White, J. (1990) *Annu. Rev. Physiol. 52*, 675−690.
61. Greene, M., Williams, D. S., and Newton, A. C. (1997) *J. Biol. Chem 16*, 10341−10344.
62. Bentz, J., and Ellens, H. (1988) *Colloids Surf. 30*, 65−112.
63. Surewicz, W. K., and Mantsch, H. H. (1988) *Biochim. Biophysc. Acta 952*, 115−130.
64. Lawless, M. K., Barney, S., Guthrie, K. I., Bucy, T. B., Petteway, S. R., and Meritka, G. (1996) *Biochemistry 35*, 13697−13708.
65. Davies, K. (1993) *Nature 362*, 92.
66. Molday, R. S. (1994) *Prog. Retinal Eye Res. 13*, 271−299.
67. Travis, G. H., and Hepler, J. E. (1993) *Nat. Genet. 3*, 191−192.
68. Connell, G., Bascom, R., Molday, L., Reid D., McInnes, R., and Molday, R. S. (1991) *Proc. Natl. Acad. Sci. U.S.A. 88*, 723−726.
69. Sanyal, S., and Jansen, H. G. (1981) *Neurosci. Lett. 21*, 23−26.
70. Bascom, R. A., Schappert, K., and McInnes, R. R. (1993) *Hum. Mol. Genet. 2*, 385−391.
71. Dryja, T. P., Hahn, L. B., Kajiwara, K., and Berson, E. (1997) *Invest. Ohpthalmol. Vis. Sci. 38*, 1972−1982.
72. Goldberg, F. X., and Molday, R. S. (1996) *Proc. Natl. Acad. Sci. U.S.A. 93*, 13726−13730.
73. Kedzierski, W., Moghrabi, W. N., Allen, A. C., Jablonski-Stiemke, M. M., Azarian, S. M., Bok, D., and Travis, G. (1996) *J. Cell Sci. 109*, 2551−2560.

BI980173P